*Inorg. Chem.* **2005**, *44*, 7122–7129


# A Series of Three-Dimensional Lanthanide Coordination Polymers with Rutile and Unprecedented Rutile-Related Topologies

**Chao Qin, Xin-Long Wang, En-Bo Wang,* and Zhong-Min Su***

*Institute of Polyoxometalate Chemistry, Department of Chemistry, Northeast Normal University, Changchun 130024, P. R. China*

Received June 5, 2005

The complexes of formulas Ln(pydc)(Hpydc) (Ln = Sm (**1**), Eu (**2**), Gd (**3**); $H_2$pydc = pyridine-2,5-dicarboxylic acid) and Ln(pydc)(bc)($H_2O$) (Ln = Sm (**4**), Gd (**5**); Hbc = benzenecarboxylic acid) have been synthesized under hydrothermal conditions and characterized by elemental analysis, IR, TG analysis, and single-crystal X-ray diffraction. Compounds **1**–**3** are isomorphous and crystallize in the orthorhombic system, space group *Pbcn*. Their final three-dimensional racemic frameworks can be considered as being constructed by helix-linked scalelike sheets. Compounds **4** and **5** are isostructural and crystallize in the monoclinic system, space group $P2_1/c$. pydc ligands bridge dinuclear lanthanide centers to form the three-dimensional frameworks featuring hexagonal channels along the *a*-axis that are occupied by one-end-coordinated bc ligands. From the topological point of view, the five three-dimensional nets are binodal with six- and three-connected nodes, the former of which exhibit a rutile-related $(4.6^2)_2(4^2\cdot6^9\cdot8^4)$ topology that is unprecedented within coordination frames, and the latter two species display a distorted rutile $(4.6^2)_2(4^2\cdot6^{10}\cdot8^3)$ topology. Furthermore, the luminescent properties of **2** were studied.

## Introduction

The crystal engineering of metal−organic frameworks (MOFs) is becoming an increasing popular field of research in view of the potential applications and unusual topologies of these new materials.[1] Much work has focused on the rational design of multidimensional infinite architectures by controlling the favored geometry of ligands and metals, in which the construction of transition-metal−carboxylate polymers is a successful paradigm.[2−4] Unfortunately, in contrast to the fruitful production of MOFs with d-block transition metal ions, the design and control over high-dimensional lanthanide-based frameworks is currently a formidable task[5] owing to coordination diversity of lanthanide ions. Whereas, lanthanides, with their high and variable coordination numbers and flexible coordination environ-

* To whom correspondence should be addressed. E-mail: wangenbo@public.cc.jl.cn (E.-B.W.).

(1) (a) Hagrman, P. J.; Hagrman, D.; Zubieta, J. *Angew. Chem., Int. Ed.* **1999**, *38*, 2638. (b) Blake, A. J.; Champness, N. R.; Hubberstey, P.; Li, W. S.; Withersby, M. A.; Schröder, M. *Coord. Chem. Rev.* **1999**, *183*, 117. (c) Moulton, B.; Zaworotko, M. J. *Chem. Rev.* **2001**, *101*, 1629. (d) Evans, O. R.; Lin, W. *Acc. Chem. Res.* **2002**, *35*, 511. (e) Yaghi, O. M.; O'Keeffe, M.; Ockwig, N. W.; Chae, H. K.; Eddaoudi, M.; Kim, J. *Nature* **2003**, *423*, 705. (f) Rao, C. N. R.; Natarajan, S.; Vaidhyanathan, R. *Angew. Chem., Int. Ed.* **2004**, *43*, 1466. (g) Kitagawa, S.; Kitaura, R.; Noro, S. I. *Angew. Chem., Int. Ed.* **2004**, *43*, 2334.

(2) (a) Lee, E.; Heo J.; Kim, K. *Angew. Chem., Int. Ed.* **2000**, *39*, 2699. (b) Halder, G. J.; Kepert, C. J.; Moubaraki, B.; Murry, K. S.; Cashion, J. D. *Science* **2002**, *298*, 1762. (c) Prior, T. J.; Bradshaw, D.; Teat, S. J.; Rosseinsky, M. J. *Chem. Commun.* **2003**, 500. (d) Ma, B. Q.; Sun, H. L.; Gao, S. *Chem. Commun.* **2003**, 2164. (e) Pan, L.; Liu, H.; Lei, X.; Huang, X.; Olson, D. H.; Turro, N. J.; Li, J. *Angew. Chem., Int. Ed.* **2003**, *42*, 542. (f) Zhang, J. P.; Lin, Y. Y.; Huang, X. C.; Chen, X. M. *J. Am. Chem. Soc.* **2005**, *127*, 5495.

(3) (a) Li, Y. H.; Su, C. Y.; Goforth, A. M.; Shimizu, K. D.; Gray, K. D.; Smith, M. D.; zur Loye, H. C. *Chem. Commun.* **2003**, 1630. (b) Wang, X. L.; Qin, C.; Wang, E. B.; Li, Y. G.; Hu, C. W.; Xu, L. *Chem. Commun.* **2004**, 378. (c) Bu, X. H.; Tong, M. L.; Chang, H. C.; Kitagawa, S.; Batten, S. R. *Angew. Chem., Int. Ed.* **2004**, *43*, 192. (d) Zhang, X. M.; Fang, R. Q.; Wu. H. S. *J. Am. Chem. Soc.* **2005**, in press. (e) Cheng, J. K.; Chen, Y. B.; Wu, L.; Zhang, J.; Wen, Y. H.; Li, Z. J.; Yao, Y. G. *Inorg. Chem.* **2005**, *44*, 3386.

(4) (a) Galet, A.; Munoz, M. C.; Real, J. A. *J. Am. Chem. Soc.* **2003**, *125*, 14224. (b) Forster, P. M.; Eckert, J.; Chang, J. S.; Park, S. E.; Férey, G.; Cheetham, A. K. *J. Am. Chem. Soc.* **2003**, *125*, 1309. (c) Liang, K.; Zheng,; Song, Y.; Lappert, M. F.; Li, Y.; Xin, X.; Huang, Z.; Chen, J.; Lu, S. *Angew. Chem., Int. Ed.* **2004**, *43*, 5776. (d) Nakabayashi, K.; Kawano, M.; Yoshizawa, M.; Ohkoshi, S. I.; Fujita, M. *J. Am. Chem. Soc.* **2004**, *126*, 16694. (e) Song, J. L.; Zhao, H. H.; Mao, J. G.; Dunbar, K. R. *Chem. Mater.* **2004**, *16*, 1884. (f) Zheng, J. M.; Batten, S. R.; Du, M. *Inorg. Chem.* **2005**, *44*, 3317.

(5) (a) Kiritsis, V.; Michaelides, A.; Skoulika, S.; Golhen, S.; Ouahab, L. *Inorg. Chem.* **1998**, *37*, 3407. (b) Reineke, T. M.; Eddaoudi, M.; Moler, D.; O'Keeffe, M.; Yaghi, O. M. *J. Am. Chem. Soc.* **2000**, *122*, 4843. (c) Pan, L.; Adams, K. M.; Hernandez, H. E.; Wang, X. T.; Zheng. C.; Hattori, Y.; Kaneko, K. *J. Am. Chem. Soc.* **2003**, *125*, 3062. (d) Zhao, B.; Cheng, P.; Chen, X. Y.; Cheng, C.; Shi, W.; Liao, D. Z.; Yan, S. P.; Jiang, Z. H. *J. Am. Chem. Soc.* **2004**, *126*, 3012. (e) Guo, X. D.; Zhu, G. S.; Fang, Q. R.; Xue, M.; Tian, G.; Sun, J. Y.; Li, X. T.; Qiu, S. L. *Inorg. Chem.* **2005**, *44*, 3850.



10.1021/ic050906b CCC: $30.25 
Published on Web 09/08/2005

ments, provide unique opportunities for discovery of unusual network topologies,[6] thus leading us to this interesting and challenging field.

The "network approach" or topological approach is a powerful tool for the analysis, comparison, and design of network structures.[7] By reducing multidimensional structures to simple node-and-connection reference nets, it plays an essential role in structural simplification and subsequent systematization. As stated by Wells, the crystallographer generally describes patterns of atoms in terms of their symmetries; namely, the description is geometrically based on lengths and angles, whereas the approach of topological is concerned with the way in which the points are connected and with the numbers of edges of the polygons.[7a] Generally, topological analysis of a crystal structure needs a simplified process; that is, remove all the unnecessary elements that have no topological relevance, leaving only the essentials, and thus the crystal structure was reduced to an irreducible net represented by points and lines linking them together.[8] The notation for 2D or 3D nets is based on the analysis of the "circuits", i.e. the shortest path which starts from a point along one link and returns to the point by another link, characterized by the number $q$ of edges in a loop. A $p$-connected node ($p$ is the number of connections to neighboring nodes that radiate from any node, the minimal value of which is 3) can be identified by a Schläfli symbol (or *point symbol*) of the type $q^a.q^b...$, where the number of circuits of each kind is shown as a superscript.[7a,9g] Network topologies in coordination polymers have already been discussed in several detailed reviews.[9] Ockwig, O'Keeffe, Yaghi, and co-workers have recently systematically analyzed the underlying topologies of all 1127 three-dimensional (3D) metal−organic frameworks reported in the Cambridge Structure Database (CSD), and the statistical results show that only 353 (31.3%) MOFs out of the 1127 refcodes have different connectivities (3,4; 3,5; 4,5; 3,6; 4,6; 5,6).[8] Therefore, a further investigation on the self-assembly of MOFs having mixed nodes, besides enriching the database of coordination polymers, will contribute to discovery of new and previously unrecognized topologies.

In this regard, we chose pyridine-2,5-dicarboxylate (pydc) as an organic spacer since this rigid molecule has proven to be able to establish bridges between metal centers.[10] Here, we report on five three-dimensional binodal nets resulting from the combination of six- and three-connecting nodes that are Ln(pydc)(Hpydc) (Ln = Sm (**1**), Eu (**2**), Gd (**3**)) with an unprecedented $(4.6^2)_2(4^2\cdot6^9\cdot8^4)$ topology and Ln(pydc)(bc)-($H_2O$) (Ln = Sm (**4**), Gd (**5**); Hbc = benzenecarboxylic acid) with a rutile $(4.6^2)_2(4^2\cdot6^{10}\cdot8^3)$ topology. A search in the Cambridge Structure Database reveals that only a 2D MOF assembled from Ln-only (Ln = lanthanides) and $pydc^{2-}$ has been reported;[11] the rest contain 3d−4f mixed metals.[12] Therefore, the five compounds reported herein represent the first three-dimensional series of a {Ln/pydc} system. Furthermore, the luminescent properties of **2** were studied.

## Experimental Section

**Materials.** All chemicals purchased were of reagent grade and used without further purification. All syntheses were carried out in 20 mL Teflon-lined autoclaves under autogenous pressure. The reaction vessels were filled to approximately 60% volume capacity. Water used in the reactions is distilled water.

**Synthesis of Sm(pydc)(Hpydc) (1).** A mixture of $Sm_2O_3$ (87 mg, 0.25 mmol), $H_2$pydc (167 mg, 1 mmol), $HNO_3$ (0.2 mL, 4 M), and water (10 mL) was heated at 140 °C for 5 days; colorless crystals of **1** were obtained when cooling to room temperature at 10 °C/h (yield: 173 mg, 72% based on Sm). Anal. Calcd for $C_{14}H_7N_2SmO_8$: C, 34.91; H, 1.47; N, 5.81. Found: C, 34.53; H, 1.25; N, 6.14. IR data (KBr, $cm^{-1}$): 3032 w, 1720 m, 1628 w, 1610 m, 1597 s, 1562 s, 1487 m, 1406 s, 1369 s, 1286 m, 1263 w, 1184 m, 1159 m, 1039 m, 904 w, 831 m, 792 m, 760 s, 693 s, 649 m, 570 m, 521 m, 436 w.

**Synthesis of Eu(pydc)(Hpydc) (2).** An identical procedure with **1** was followed to prepare **2** except $Sm_2O_3$ was replaced by $Eu_2O_3$ (88 mg, 0.25 mmol) (yield: 181 mg, 75% based on Eu). Anal. Calcd for $C_{14}H_7N_2EuO_8$: C, 34.80; H, 1.46; N, 5.79. Found: C, 34.55; H, 1.62; N, 5.38. IR data (KBr, $cm^{-1}$): 3029 w, 1718 m, 1630 w, 1592 w, 1570 s, 1485 s, 1406 s, 1372 s, 1300 m, 1280 w, 1185 m, 1045 m, 1036 m, 904 w, 835 m, 791 m, 767 s, 686 s, 650 m, 529 s, 428 w.

**Synthesis of Gd(pydc)(Hpydc) (3).** An identical procedure with **1** was followed to prepare **3** except $Sm_2O_3$ was replaced by $Gd_2O_3$ (91 mg, 0.25 mmol) (yield: 171 mg, 70% based on Gd). Anal. Calcd for $C_{14}H_7N_2GdO_8$: C, 34.42; H, 1.44; N, 5.73. Found: C, 34.79; H, 1.26; N, 5.70. IR data (KBr, $cm^{-1}$): 3037 w, 1715 m, 1632 w, 1610 m, 1560 s, 1490 s, 1400 s, 1369 s, 1284 m, 1243 w,


(6) (a) Long, D. L.; J. Blake, A.; Champness, N. R.; Wilson, C.; Schröder, M. *Angew. Chem., Int. Ed.* **2001**, *40*, 2443. (b) Long, D. L.; Hill, R. J.; Blake, A. L.; Champness, N. R.; Hubberstey, P.; Proserpio, D. M.; Wilson, C.; Schröder, M. *Angew. Chem., Int. Ed.* **2004**, *43*, 1851. (c) Cui, Y.; Ngo, H. L.; White, P. S.; Lin, W. *Chem. Commun.* **2002**, 1666. (d) Almeida Paz, F. A.; Klinowski, J. *Chem. Commun.* **2003**, 1484. (e) Ren, Y. P.; Long, L. S.; Mao, B. W.; Yuan, Y. Z.; Huang, R. B.; Zheng, L. S. *Angew. Chem., Int. Ed.* **2003**, *42*, 532. (f) Zheng, X. J.; Sun, C. Y.; Lu, S. Z.; Liao, F. H.; Gao, S.; Jin, L. P. *Eur. J. Inorg. Chem.* **2004**, 3262. (g) Zhang, M. B.; Zhang, J.; Zheng, S. T.; Yang, G. Y. *Angew. Chem., Int. Ed.* **2005**, *44*, 1385.

(7) (a) Wells, A. F. *Further studies of three-dimensional nets*; American Crystallographic Association (distributed by Polycrystal Book Service): New York (Pittsburgh, PA), 1979. (b) Wells, A. F. *Threedimensional nets and polyhedra*; Wiley: New York, 1977. (c) Blake, A. J.; Champness, N. R.; Hubberstey, P.; Li, W. S.; Withersby, M. A.; Schröder, M. *Coord. Chem. Rev.* **1999**, *183*, 117. (d) Friedrichs, O. D.; O'Keeffe M.; Yaghi, O. M. *Acta Crystallogr., Sect. A* **2003**, *59*, 22.

(8) Ockwig, N. W.; Delgado-Friederichs, O.; O'Keeffee, M.; Yaghi, O. M. *Acc. Chem. Res*. **2005**, *38*, 176.

(9) (a) Han S.; Smith, J. V. *Acta Crystallogr*. **1999**, *A55*, 322. (b) Robson, R.; *J. Chem. Soc., Dalton Trans*. **2000**, 3735. (c) O'Keeffe, M.; Eddaoudi, M.; Li, H.; Reineke, T.; Yaghi, O. M. *J. Solid State Chem.* **2000**, *152*, 3. (d) Batten, S. R. *CrystEngComm* **2001**, *3*, 67. (e) Biradha, K. *CrystEngComm* **2003**, *5*, 374. (f) Barnett S. A.; Champness, N. R. *Coord. Chem. Rev.* **2003**, *246*, 145. (g) Carlucci, L.; Ciani, G.; Proserpio, D. M. *Coord. Chem. Rev.* **2003**, *246*, 247. (h) Blatov, V. A.; Carlucci, L.; Ciani, G.; Proserpio, D. M. *CrystEngComm* **2004**, *6*, 377.

(10) (a) Min, D.; Yoon, S. S.; Jung, D. Y.; Lee, C. Y.; Kim, Y.; Han, W. S.; Lee, S. W. *Inorg. Chim. Acta* **2001**, *324*, 293. (b) García-Zarracino, R.; Höpfl, H. *Angew. Chem., Int. Ed.* **2004**, *43*, 1507. (c) Humphrey, S. M.; Wood, P. T. *J. Am. Chem. Soc.* **2004**, *126*, 13236. (d) Liu, Y. L.; Kravtsov, V. C.; Beauchamp, D. A.; Eubank, J. F.; Eddaoudi, M. *J. Am. Chem. Soc.* **2005**, *127*, 7266. (e) Wei, Y. L.; Hou, H. W.; Li, L. K.; Fan, Y. T.; Zhou, Y. *Cryst. Growth Des.* **2005**, *15*, 1405.

(11) Zhang, X. F.; Huang, D. G.; Chen, C. N.; Liu, Q. T.; Liao, D. Z.; Li, L. C. *Inorg. Chem. Commun.* **2005**, *8*, 22.

(12) (a) Liang, Y.; Cao, R.; Su, W. P.; Hong, M. C.; Zhang, W. J. *Angew. Chem., Int. Ed.* **2000**, *39*, 3304. (b) Liang, Y. C.; Hong, M. C.; Su, W. P.; Cao R.; Zhang, W. J. *Inorg. Chem.* **2001**, *20*, 4574.

**Table 1.** Crystal Data and Structure Refinement for **1**−**5**

| param | **1** | **2** | **3** | **4** | **5** |
|---|---|---|---|---|---|
| empirical formula | $C_{14}H_7N_2SmO_8$ | $C_{14}H_7N_2EuO_8$ | $C_{14}H_7N_2GdO_8$ | $C_{14}H_{10}NSmO_7$ | $C_{14}H_{10}NGdO_7$ |
| *M* | 481.57 | 483.18 | 488.47 | 454.58 | 461.48 |
| *T*/K | 293(2) | 293(2) | 293(2) | 293(2) | 293(2) |
| $\lambda$/Å | 0.710 73 | 0.710 73 | 0.710 73 | 0.710 73 | 0.710 73 |
| cryst system | orthorhombic | orthorhombic | orthorhombic | monoclinic | monoclinic |
| space group | Pbcn | Pbcn | Pbcn | $P2_1/c$ | $P2_1/c$ |
| *a*/Å | 9.939(2) | 9.969(2) | 9.932(2) | 9.2735(19) | 9.2498(18) |
| *b*/Å | 8.6219(17) | 8.6644(17) | 8.6161(17) | 14.244(3) | 14.169(3) |
| *c*/Å | 15.731(3) | 15.736(3) | 15.717(3) | 10.579(2) | 10.514(2) |
| α/deg | 90 | 90 | 90 | 90 | 90 |
| $\beta$/deg | 90 | 90 | 90 | 95.65(3) | 95.77(3) |
| $\gamma$/deg | 90 | 90 | 90 | 90 | 90 |
| *V*/Å$^3$ | 1348.0(5) | 1359.3(5) | 1344.9(5) | 1390.6(5) | 1371.0(5) |
| *Z* | 4 | 4 | 4 | 4 | 4 |
| $\mu$/mm$^{-1}$ | 4.411 | 4.669 | 4.986 | 4.261 | 4.877 |
| $R_1$[a] [$I > 2\sigma(I)$] | 0.0172 | 0.0204 | 0.0166 | 0.0272 | 0.0255 |
| $wR_2$[b] | 0.0375 | 0.0407 | 0.0338 | 0.0557 | 0.0478 |

[a] $R_1 = \Sigma||F_o| - |F_c||/\Sigma|F_o|$. [b] $wR_2 = \Sigma[w(F_o^2 - F_c^2)^2]/\Sigma[w(F_o^2)^2]^{1/2}$.

1178 m, 1138 m, 1038 m, 882 w, 845 m, 792 m, 760 s, 696 s, 652 m, 578 m, 525 s, 432 w.

**Synthesis of Sm(pydc)(bc)($H_2O$) (4).** A mixture of $Sm_2O_3$ (87 mg, 0.25 mmol), $H_2$pydc (84 mg, 0.5 mmol), Hbc (61 mg, 0.5 mmol), $HNO_3$ (0.10 mL, 4 M), and water (10 mL) was heated at 140 °C for 5 days; colorless crystals of **4** were obtained when cooling to room temperature at 10 °C/h (yield: 177 mg, 78% based on Sm). Anal. Calcd for $C_{14}H_{10}NSmO_7$: C, 36.99; H, 2.21; N, 3.08. Found: C, 36.52; H, 2.27; N, 3.41. IR data (KBr, cm$^{-1}$): 3222 m, br, 3073 w, 3047 w, 1665 s, 1602 m, 1592 s, 1579 s, 1482 m, 1432 s, 1414 w, 1394 s, 1363 s, 1283 m, 1172 m, 1034 s, 821 s, 771 s, 698 m, 680 w, 651 w, 507 m, 432 m.

**Synthesis of Gd(pydc)(bc)($H_2O$) (5).** An identical procedure with **4** was followed to prepare **5** except $Sm_2O_3$ was replaced by $Gd_2O_3$ (91 mg, 0.25 mmol) (yield: 189 mg, 82% based on Gd). Anal. Calcd for $C_{14}H_{10}NGdO_7$: C, 36.43; H, 2.18; N, 3.03. Found: C, 36.74; H, 2.32; N, 2.75. IR data (KBr, cm$^{-1}$): 3220 m, br, 3070 w, 3044 w, 1660 s, 1603 m, 1594 s, 1586 s, 1480 m, 1432 s, 1416 w, 1397 s, 1363 s, 1280 m, 1198 m, 1048 s, 823 s, 770 s, 755 m, 724 m, 683 m, 654 w, 509 m, 434 m.

**X-ray Crystallography.** Single crystals of compounds **1**−**5** were glued on a glass fiber. Data were collected on a Rigaku R-AXIS RAPID IP diffractometer with Mo Kα monochromated radiation ($\lambda$ = 0.710 73 Å) at 293 K. Empirical absorption correction was applied. The structures were solved by the direct method and refined by the full-matrix least-squares methods on $F^2$ using the SHELXTL crystallographic software package.[13] Anisotropic thermal parameters were used to refine all non-hydrogen atoms. The hydrogen atoms were included at idealized positions, and the H(4) atom of compounds **1**−**3** is modeled with 50% occupancy. The crystal data and structure refinement of compounds **1**−**5** are summarized in Table 1. Selected bond lengths and angles for **1**−**5** are listed in Table 2.

**Physical Measurements.** Elemental analyses (C, H, and N) were performed on a Perkin-Elmer 2400 CHN elemental analyzer. FTIR spectra were recorded in the range 400−4000 cm$^{-1}$ on an Alpha Centaurt FTIR spectrophotometer using a KBr pellet. TG-DTA measurements were performed on a Perkin-Elmer TGA7 instrument in flowing $N_2$ with a heating rate of 10 °C min$^{-1}$. Excitation and

**Table 2.** Selected Bond Lengths (Å) and Angles (deg) for **1**−**5**[a]

| | | | |
|---|---|---|---|
| | Compound **1** | | |
| Sm(1)−O(2A) | 2.3503(17) | Sm(1)−O(3D) | 2.4075(18) |
| Sm(1)−O(2B) | 2.3503(17) | Sm(1)−O(3E) | 2.4075(18) |
| Sm(1)−O(1C) | 2.3754(17) | Sm(1)−N(1C) | 2.5851(19) |
| Sm(1)−O(1) | 2.3755(17) | Sm(1)−N(1) | 2.5852(19) |
| O(1)−Sm(1)−O(3D) | 109.40(6) | O(3E)−Sm(1)−N(1C) | 155.35(6) |
| O(2B)−Sm(1)−O(1) | 74.45(7) | O(1)−Sm(1)−N(1) | 64.95(6) |
| O(2B)−Sm(1)−O(3D) | 76.45(6) | O(2A)−Sm(1)−N(1) | 123.66(6) |
| O(2A)−Sm(1)−O(1) | 146.40(6) | O(2B)−Sm(1)−N(1) | 78.95(6) |
| | Compound **2** | | |
| Eu(1)−O(2A) | 2.350(2) | Eu(1)−O(3D) | 2.405(2) |
| Eu(1)−O(2B) | 2.350(2) | Eu(1)−O(3E) | 2.405(2) |
| Eu(1)−O(1C) | 2.384(2) | Eu(1)−N(1) | 2.581(2) |
| Eu(1)−O(1) | 2.384(2) | Eu(1)−N(1C) | 2.581(2) |
| O(2B)−Eu(1)−O(1) | 74.59(8) | O(2A)−Eu(1)−N(1) | 123.54(7) |
| O(2A)−Eu(1)−O(1) | 146.55(7) | O(1C)−Eu(1)−N(1) | 70.43(7) |
| O(2A)−Eu(1)−O(3D) | 75.19(8) | O(1)−Eu(1)−N(1) | 65.17(7) |
| O(1)−Eu(1)−O(3D) | 109.20(7) | O(3E)−Eu(1)−N(1) | 75.35(7) |
| | Compound **3** | | |
| Gd(1)−O(2A) | 2.3379(17) | Gd(1)−O(3D) | 2.3877(17) |
| Gd(1)−O(2B) | 2.3379(17) | Gd(1)−O(3E) | 2.3877(17) |
| Gd(1)−O(1) | 2.3697(16) | Gd(1)−N(1) | 2.5693(18) |
| Gd(1)−O(1C) | 2.3697(16) | Gd(1)−N(1C) | 2.5693(18) |
| O(2A)−Gd(1)−O(1) | 146.75(6) | O(1)−Gd(1)−N(1) | 65.48(5) |
| O(2B)−Gd(1)−O(1) | 74.53(6) | O(2A)−Gd(1)−N(1) | 123.36(6) |
| O(1)−Gd(1)−O(1C) | 80.37(8) | O(3D)−Gd(1)−N(1) | 155.34(6) |
| O(1)−Gd(1)−O(3D) | 108.80(6) | O(3D)−Gd(1)−N(1C) | 75.08(6) |
| | Compound **4** | | |
| Sm(1)−O(6A) | 2.330(3) | Sm(1)−O(1W) | 2.428(3) |
| Sm(1)−O(5) | 2.390(3) | Sm(1)−O(1) | 2.467(3) |
| Sm(1)−O(3B) | 2.389(3) | Sm(1)−O(2D) | 2.467(3) |
| Sm(1)−O(4C) | 2.413(3) | Sm(1)−N(1) | 2.628(3) |
| O(6A)−Sm(1)−O(5) | 119.87(11) | O(1)−Sm(1)−O(2D) | 108.16(9) |
| O(6A)−Sm(1)−O(1) | 149.23(10) | O(5)−Sm(1)−N(1) | 71.38(10) |
| O(5)−Sm(1)−O(4C) | 72.80(11) | O(6A)−Sm(1)−N(1) | 146.89(10) |
| O(5)−Sm(1)−O(1W) | 140.22(10) | O(1W)−Sm(1)−N(1) | 111.63(11) |
| O(1W)−Sm(1)−O(2D) | 72.14(9) | O(1)−Sm(1)−N(1) | 62.58(9) |
| O(1W)−Sm(1)−O(1) | 77.14(10) | O(2D)−Sm(1)−N(1) | 71.54(9) |
| | Compound **5** | | |
| Gd(1)−O(5) | 2.304(3) | Gd(1)−O(1W) | 2.397(3) |
| Gd(1)−O(6A) | 2.358(3) | Gd(1)−O(2D) | 2.442(2) |
| Gd(1)−O(3B) | 2.366(2) | Gd(1)−O(1) | 2.443(3) |
| Gd(1)−O(4C) | 2.385(3) | Gd(1)−N(1) | 2.601(3) |
| O(5)−Gd(1)−O(6A) | 119.44(11) | O(4C)−Gd(1)−O(1) | 132.66(9) |
| O(6A)−Gd(1)−O(1) | 70.12(10) | O(6A)−Gd(1)−N(1) | 72.01(10) |
| O(1W)−Gd(1)−O(1) | 76.56(10) | O(4C)−Gd(1)−N(1) | 78.08(10) |
| O(5)−Gd(1)−O(1W) | 80.47(12) | O(5)−Gd(1)−N(1) | 146.64(10) |
| O(5)−Gd(1)−O(1) | 148.70(10) | O(1W)−Gd(1)−N(1) | 111.24(11) |
| O(3B)−Gd(1)−O(1) | 76.32(9) | O(1)−Gd(1)−N(1) | 63.27(9) |

[a] Symmetry codes follow. For **1**−**3**: (A) $x - 1/2$, $y - 1/2$, $-z + 1/2$; (B) $-x + 1/2$, $y - 1/2$, $z$; (C) $-x$, $y$, $-z + 1/2$; (D) $x$, $-y$, $z - 1/2$; (E) $-x$, $-y$, $-z + 1$. For **4**: (A) $-x$, $-y$, $-z + 1$; (B) $x - 1$, $y$, $z$; (C) $-x + 1$, $-y$, $-z + 1$; (D) $x$, $-y + 1/2$, $z - 1/2$. For **5**: (A) $-x + 1$, $-y$, $-z$; (B) $x + 1$, $y$, $z$; (C) $-x$, $-y$, $-z$; (D) $x$, $-y - 1/2$, $z + 1/2$.

(13) (a) Sheldrick. G. M. *SHELXS97. A Program for the Solution of Crystal Structures from X-ray Data*; University of Göttingen: Göttingen, Germany, 1997. (b) Sheldrick, G. M. *SHELXL97. A Program for the Refinement of Crystal Structures from X-ray Data*; University of Göttingen: Göttingen, Germany, 1997.

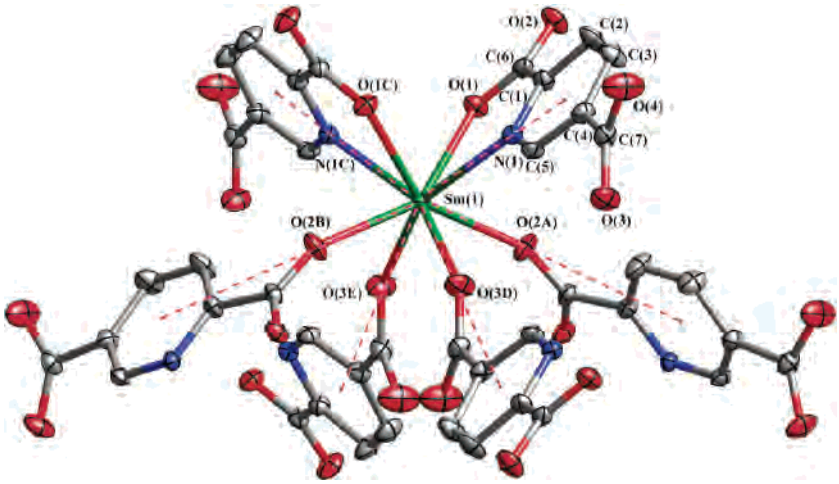


**Figure 1.** ORTEP representation of atom numbering diagram for **1** (50% probability ellipsoids). Dashed lines illustrate the six-connected circumstance of the Sm node.

**Chart 1** Representations of the Observed Coordination Modes a−k of pydc[a]

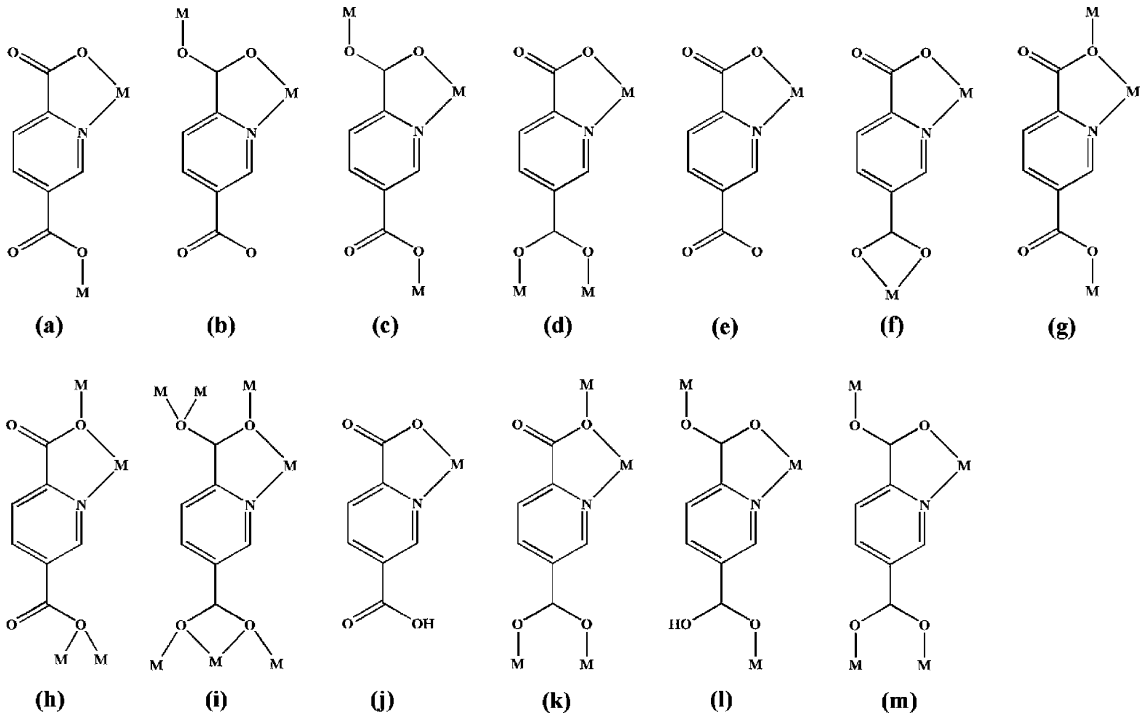


[a] Two new coordination modes in this paper are shown as modes l and m.

emission spectra were obtained on a SPEX FL-2T2 spectrofluorometer equipped with a 450 W xenon lamp as the excitation source.

## Results and Discussion

**Synthesis and Characterization.** We tried to isolate these single crystals from a conventional solution method using the reactions of lanthanide nitrate with pydc; unfortunately, only uncharacterized white precipitates insoluble in most common solvents were obtained. Hydrothermal reactions in the presence of organic molecules have been established as powerful methods for the isolation of new materials with diverse structural architectures[14] in that at the higher temperature the reaction becomes faster thus leading to a higher

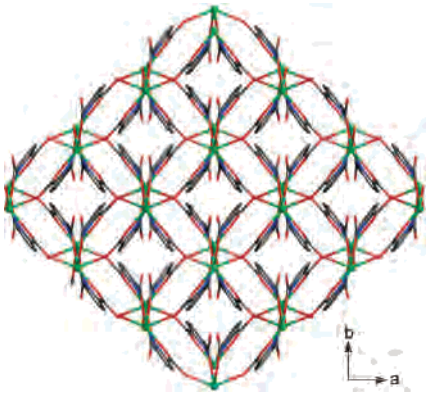


**Figure 2.** Intricate three-dimensional structure of **1** viewed down the *c* axis.

(14) Feng, S. H.; Xu, R. R. *Acc. Chem. Res.* **2001**, *34*, 239.

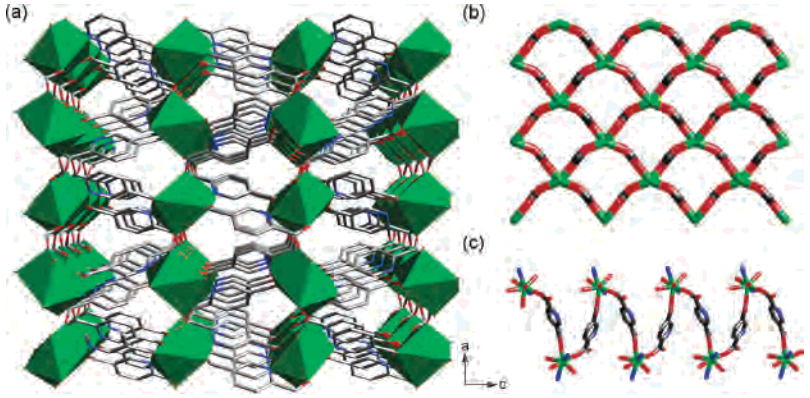


**Figure 3.** (a) Perspective view of the three-dimensional network of **1** constructed by the helix-linked scalelike sheets running along the *b* axis. (b) View of a scalelike ···Sm−O−C−O−Sm··· sheet. (c) Helical chain formed by Sm atoms and pydc ligands.

degree of reversibility in the process of crystal growth that is likely to encourage the generation of larger crystals. After introducing hydrothermal methods, we obtained a small quantity of microlite unsuitable for single-crystal X-ray diffraction starting from the same reaction materials. Although detailed studies are still needed, we sense that changing lanthanide sources may be helpful for the crystal growth. In view of this, we replaced lanthanide salts with lanthanide oxides, accompanied with adding dilute $HNO_3$, hoping lanthanide ions could be slowly released during action with $HNO_3$ so as to lower the polymerization rate. As expected, when the reactions of $Ln_2O_3$ and pydc were carried out at 140 °C for 5 days under hydrothermal conditions, well-formed single crystals of **1**−**5** were obtained in satisfying yields.

The IR spectra show features attributable to the carboxylate stretching vibrations of the complexes. For **1**−**3**, the characteristic bands of carboxylate groups are shown in the range 1560−1632 $cm^{-1}$ for asymmetric stretching and 1370−1490 $cm^{-1}$ for symmetric stretching. The characteristic bands observed for **1**−**3** at around 1700 $cm^{-1}$ attributed to the protonated carboxylic groups indicate the incomplete deprotonation of $H_2$pydc ligands. For **4** and **5**, the signals in the range 1580−1665 $cm^{-1}$ can be assigned to the asymmetric stretching vibrations for the carboxylate groups, and the signals between 1360 and 1482 $cm^{-1}$ correspond to the symmetric stretching vibrations. The bands in the region ca. 650−1300 $cm^{-1}$ for **1**−**5** can be assigned to the CH in-plane or out-of-plane bend, ring breathing, and ring deformation absorptions of pyridine ring. Weak absorptions observed at 3033−3075 $cm^{-1}$ for **1**−**5** can be attributed to the $\nu_{C-H}$ of the pyridyl. The broad bands at ca. 3200 $cm^{-1}$ for **4** and **5** are attributed to the vibrations of water ligand.

**Crystal Structures. Ln(pydc)(Hpydc) [1 (Ln = Sm), 2 (Ln = Eu), and 3 (Ln = Gd)].** Since **2** and **3** are isomorphous with **1**, the structure of **1** is described representatively. An atom numbering diagram of the fundamental unit for **1** is shown in Figure 1. **1** crystallizes in the orthorhombic system, space group *Pbcn*. There is a crystallographically independent samarium ion in this structure. The local coordination geometry for the eight-coordinate Sm(1) center is close to a trigonal dodecahedron coordinated by six oxygen atoms and two nitrogen atoms from six pydc ligands. This, therefore, defines a six-connecting node within the structure. The Sm−O(carboxylate) bond distances range from 2.3503(17) to 2.4075(18) Å, while the Sm−N band length is slightly longer, 2.5851(19) Å. Similar trends are observed for **2** and **3**. The coordination modes of pydc in structurally characterized coordination polymers observed up to now are summarized in Chart 1. As can be seen, the nitrogen and one of the 2-carboxylate oxygen atoms prefer to chelate one metal atom, and the 5-carboxyl group tends to ligate a metal in a bidentate or monodentate fashion or even be free. pydc in **1** adopts a new coordination fashion, shown in Chart 1. Besides linking three metal atoms, deprotonation of $H_2$pydc ligand is incomplete, which can be verified by the presence of characteristic bands at about 1700 $cm^{-1}$ in IR spectrum.[15] And thus, each pydc ligand affords a three-connecting node. The Sm centers are interconnected through pydc ligands to generate an intricate three-dimensional architecture with a wide range of C−O−Sm angles (125.9−154.9°) and C−N−Sm angles (115.8−126.3°), as shown in Figure 2. Viewed along the *b* axis, the detailed links can be described stepwise: the Sm centers are first linked by a nitrogen atom and 2-carboxylate groups to

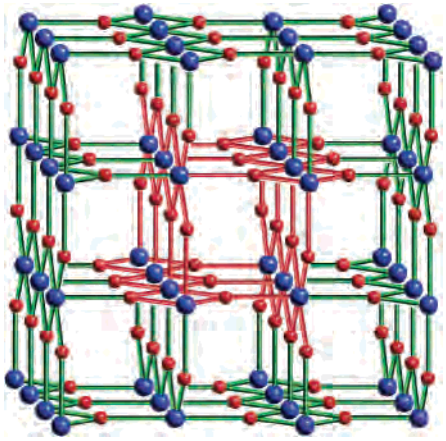

**Figure 4.** Rutile ($TiO_2$) framework. Six-connecting nodes (Ti) are represented by large balls, and three-connecting nodes (O) are represented by small balls. A square channel constructed by cross-linking $TiO_2$ chains is highlighted in the center in which the three-connecting centers act as the sides of the channels and the six-connecting centers occupy the corners.

(15) Bellamy, L. J. *The Infrared Spectra of Complex Molecules*; Wiley: New York, 1958.

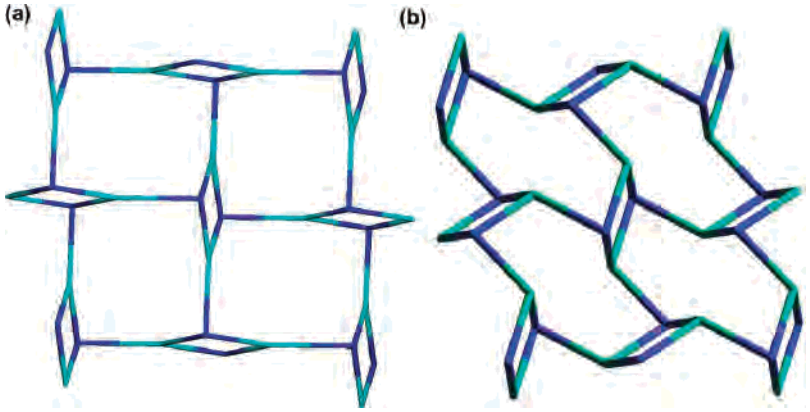


**Figure 5.** Three-connected subnets with the topology of $4.8^2$ in a prototypical lattice of rutile (a) and **1** (b).

form a scalelike ···Sm−O−C−O−Sm··· sheet (see Figure 3b), and then these sheets are further cross-linked by $C_5$-$NH_3$ spacers of pydc anions via 5-carboxlyate groups into the three-dimensional structure (Figure 3a). Very intriguingly, a careful examination shows that in the interlayer regions there exist parallel helical chains, which are formed by pydc ligands bridging samarium atoms along the crystallographic $2_1$-axis with a pitch of 9.939(2) Å (see Figure 3c). The rotation directions of helices between two adjacent sheets are just opposite; therefore, the final three-dimensional racemic framework can be considered as being constructed by helix-linked scalelike sheets. Moreover, it is interesting to note that two symmetry-related O4 atoms near each Sm are very close to each other (2.401(3) Å). On this basis, the missing H atom would appear to be disordered over two sites between the two atoms. And thus with the Sm center between O3E and O3D (see Figure 1) a hydrogen-bonded ring O3−Sm−O3−C7−O4−H···O4−C7−O3 is formed, which resembles the hydrogen-bonded ring in the acetic acid dimer. These intramolecular hydrogen-bonding interactions play important roles in stabilizing the uncoordinated carboxyl oxygen atoms and the whole 3D structure.

A better insight into the nature of this intricate framework can be achieved by the application of topological approach, i.e. reducing multidimensional structures to simple node-and-connection nets. As discussed above, the structure of **1** is binodal with six-connected (Sm atom) and three-connected (pydc ligand) nodes. However, it does not exhibit the most probable prototypical reference network—rutile (see Figure 4)—as expected to be with these types of centers, but adopts an unprecedented $(4.6^2)_2(4^2{\cdot}6^9{\cdot}8^4)$ topology (the first symbol for pydc ligand, the second one for Sm atom). To our knowledge, it is completely new within coordination polymer chemistry, and the finding of this new topology is useful at the basic level in the crystal engineering of coordination networks. The Schläfli notation, as we can seen, is different but closely related to rutile $(4.6^2)_2(4^2{\cdot}6^{10}{\cdot}8^3)$. If we look at an alternative view of the 3D network of **1** to imagine taking it apart, the similarities and differences of the new network to rutile become apparent. First, for a single 3D rutile framework, it can be separated into sets of isolated segments as shown in Figure 5a, each corresponding to a three-connected subnet with the topology of $4.8^2$. These subnets

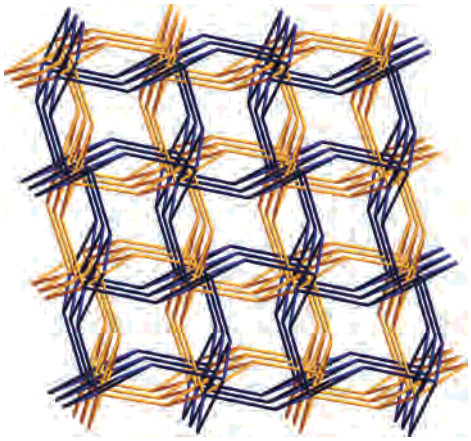

**Figure 6.** Schematic illustrating the $(4.6^2)_2(4^2{\cdot}6^9{\cdot}8^4)$ topology of the 3D network of **1**. Alternatively intersecting subnets at an angle of ca. 46.8° are highlighted in different colors.

are parallelly fused together in an AAAA stacking sequence by sharing metal centers to form a single rutile net, and six-membered rings are consequently formed. In the same way, the complicated 3D network of **1** can also be considered as being constructed by the similar independent subnets (see Figure 5b). However, an essential difference is that these subnets are alternately superposed in such a way that adjoining subnets intersect at an incline angle of ca. 46.8° in an ABAB sequence via sharing metal centers. As a result of this orientation mode, the topology of the material changes from $(4.6^2)_2(4^2{\cdot}6^{10}{\cdot}8^3)$ to $(4.6^2)_2(4^2{\cdot}6^9{\cdot}8^4)$ (see Figure 6). From the topological symbol it can be seen that the number of six-membered circuits around a six-connecting node decreases while the number of eight-membered circuits correspondingly increases in **1**. Moreover, due to the unique arrangement of these subnets, not only do the four-membered rings in each chain not fall on a plane as in rutile (see Figure S1) but also the interconnected four chains do not generate square channels.

**Ln(pydc)(bc)($H_2O$) [4 (Ln = Sm) and 5 (Ln = Gd)].** Atom numbering schemes for the isostructural **4** and **5** are represented by that of **4** shown in Figure 7. The Sm(III) atom exhibits a distorted triangle−dodecahedral configuration coordinated by six oxygen atoms from four pydc and two bc ligands (Sm−O 2.330(3)−2.468(3) Å), one nitrogen atom from one pydc ligand (Sm−N 2.628(3) Å), and one aqua

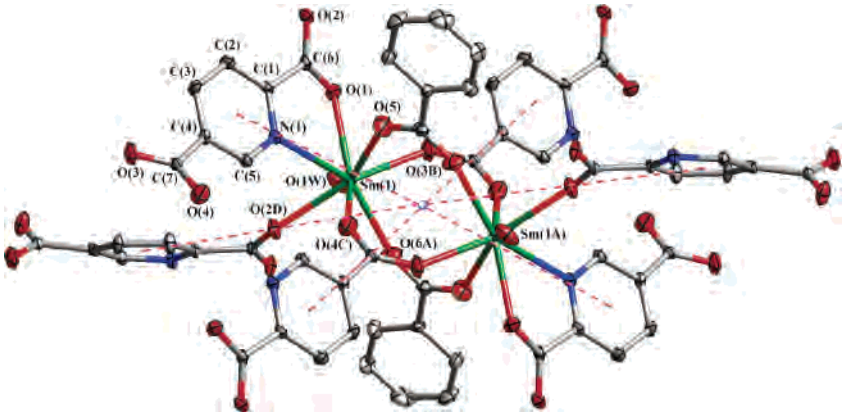


**Figure 7.** ORTEP representation of atom numbering diagram for **4** (50% probability ellipsoids). Dashed lines illustrate the six-connected circumstance of bimetallic core.

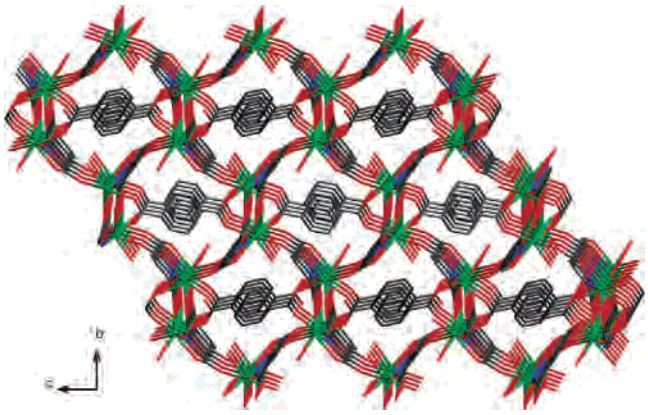

**Figure 8.** Perspective view of the three-dimensional structure of **4** along the *a*-axis, showing the one-dimensional hexagonal channels occupied by one-end-coordinated bc ligands.

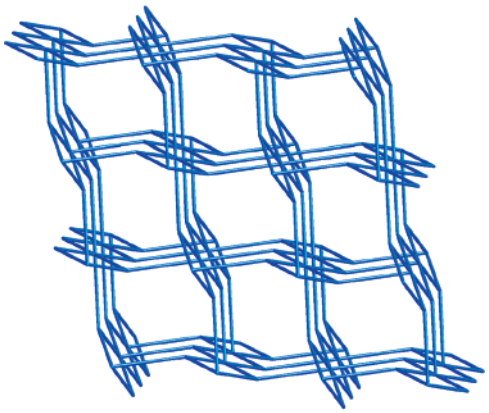

**Figure 9.** Schematic view of the deformed rutile topology of **4**.

ligand (Sm−$O_{aqua}$ 2.428(3) Å). The O−Sm−O bond angles range from 72.14(9) to 149.23(10)°, and O−Sm−N bond angles range from 62.58(9) to 146.89(10)° (see Table 2). The coordination mode of pydc in **4** is shown in Chart 1m that has not been observed before. Different from that of **1**, the 5-carboxylate bridges two metal atoms in a carboxylate O,O′ mode. The bc ligand adopts a bridging bidentate coordination mode. These bridging bidentate ends of carboxylate ligands contribute to the formation of dinuclear units, and thus, two crystallographically identical samarium ions are bridged by four pairs of $\mu_2$-carboxylate ends into a dinuclear unit with Sm···Sm distance of 4.525 Å. Each binuclear unit is further extended by the bridging pydc ligands into a three-dimensional network. Interestingly, when viewed along *a*-axis the three-dimensional network contains one-dimensional hexagonal channels that are occupied by one-end-coordinated bc ligands (see Figure 8 and Figure S2).

As shown in Figure 7, one dinuclear unit is surrounded by 10 molecules, i.e. 6 pydc, 2 bc, and 2 aqua ligands. Being end-capping units, two bc and two aqua ligands are disregarded from a topological perspective; this, therefore, defines the bimetallic core as a six-connected node. Likewise, although a pydc ligand ligates with four lanthanide ions, it actually serves as a three-connected node because two metal atoms bridged by 5-carboxlate constitute a bimetallic core and should be considered as one. On the basis of the above simplification principle, the resulting structure of compound **4** is an interesting mineralomimetic network containing alternating six-connected (bimetallic core) and three-connected nodes (pydc ligand) with the topology of $(4.6^2)_2(4^2 \cdot 6^{10} \cdot 8^3)$, which is a deformed version of the idealized rutile structure (see Figure 9). As can be seen, the adjacent chains are mutually inclined at an angle of ca. 45.8° rather than perpendicular as shown in the rutile prototype ($TiO_2$).

Recently, multicarboxylate ligands have been employed to construct lanthanide coordination polymers. In general, the greater the effective coordination sites of a carboxylate ligand, the higher the dimensionality of the resulting Ln−carboxylate network would be. To understand this, it is instructive to compare compounds **1**−**5** with other related compounds on the basis of lanthanides and carboxylic acids. As evidenced in reported complexes $[Ln(Hpdc)(H_2pdc)(H_2O)_2]$[16] (Ln = Er, Lu; $H_3pdc$ = 3,5-pyrazoledicarboxylic acid) and $[\{Nd_2(pydc)_2(Hpydc)_2(H_2O)_4\}\cdot 2H_2O]_n$,[11] the resulting architectures are both 2D rather than 3D as reported herein. The analysis for the coordination modes of carboxylate ligands reveals that this can be due to the fact that a completely free carboxyl group exists in both cases that neither is deprotonated nor takes part in coordination, thus preventing spatial extension of skeleton to higher dimensions. In addition, different from the previously reported 3D

(16) Pan, L.; Huang, X. Y.; Li, J.; Wu, Y. G.; Zheng, N. W. *Angew. Chem., Int. Ed.* **2000**, *39*, 527.

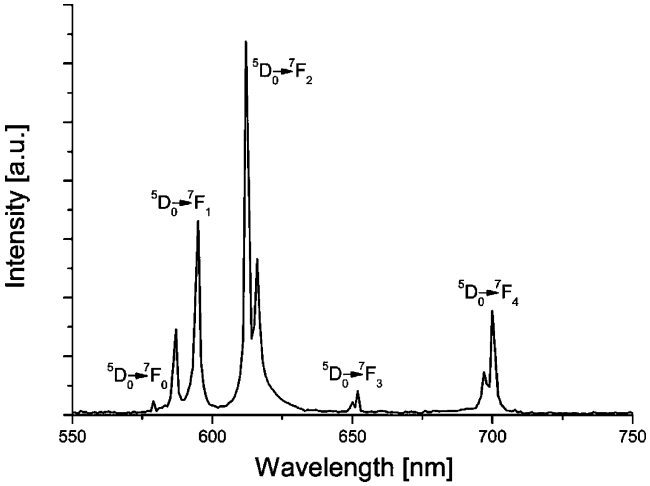


**Figure 10.** Solid-state emission spectrum for **2** at room temperature (excited at 364 nm).

lanthanide−carboxylate coordination polymers, such as [Er(CTC)($H_2O$)]·2.5$H_2O$ (CTC = *cis*,*cis*-1,3,5-cyclohexanetricarboxylate),[17] [$Yb_2$(NDC)$_3$($H_2O$)·($H_2O$)$_2$] (NDC = 2,6-naphthalenedicarboxylate),[6d] [$Eu_4$(NDC)$_6$($H_2O$)$_5$]·3$H_2O$,[6f] and Ln(bpdc)$_{1.5}$($H_2O$)·0.5DMF (bpdc = 4,4′-biphenyldicarboxylate),[5e] no solvent molecule is directly connected to the frameworks of compounds **1**−**3** due to the inherent steric hindrance of six different pydc ligands coordinated to each Ln center, which would be a useful feature to produce functional luminescent materials considering the quenching effect of −OH oscillators on luminescence.[6d,18]

**Luminescent Properties.** Taking into account the excellent luminescent properties of $Eu^{3+}$, the luminescence of **2** containing a europium ion was investigated. The emission spectrum of **2** (Figure 10) at room temperature upon excitation at 364 nm exhibits the characteristic transition of $Eu^{3+}$ ion. They are attributed to $^5D_0 \rightarrow ^7F_J$ ($J$ = 0, 1, 2, 3, 4) transitions, i.e. 580 nm ($^5D_0 \rightarrow ^7F_0$), 587 and 595 nm ($^5D_0 \rightarrow ^7F_1$), 612 and 616 nm ($^5D_0 \rightarrow ^7F_2$), 650 and 652 nm ($^5D_0 \rightarrow ^7F_3$), and 697 and 700 nm ($^5D_0 \rightarrow ^7F_4$). The most intense transition is $^5D_0 \rightarrow ^7F_2$, which implies red emission light of **2**.

## Conclusions

Reaction of lanthanide ions with pydc anions results in the formation of five three-dimensional polymeric species having different connectivities. The two new coordination modes adopted by pydc anion further reveal the versatility of pydc anions as bridging ligands. From the topological point of view, though they all contain six-connecting metal centers and three-connecting ligand centers, the former cases (**1**−**3**), as already point out, do not exhibit the most probable prototypical reference network—rutile—as expected to be with these types of centers, but adopt an unprecedented $(4.6^2)_2(4^2{\cdot}6^9{\cdot}8^4)$ topology, implying the diversification of topological connectivity and highlighting the difficulty in predicting crystal structures with certainty.

**Acknowledgment.** We thank Prof. Chunshan Shi for helpful discussions on luminescence. Special thanks are offered to three reviewers for their constructive suggestions. This work was financially supported by the National Natural Science Foundation of China (Grant No. 20371011).

**Supporting Information Available:** Additional figures, TGA and DTA curves, and X-ray crystallographic information files (CIF) for **1**−**5**. This material is available free of charge via the Internet at http://pubs.acs.org.

IC050906B

(17) Pan, L.; Woodlock, E. B.; Wang, X. T. *Inorg. Chem.* **2000**, *39*, 4174.
(18) (a) Horrocks, W. D., Jr.; Albin, M. *Prog. Inorg. Chem.* **1984**, *31*, 1. (b) Reineke, T. M.; Eddaoudi, M.; Fehr, M.; Kelley, D.; Yaghi, O. M. *J. Am. Chem. Soc.* **1999**, *121*, 1651.